Interaction Mechanisms studies of 1H-tetrazole derivatives and nitrocellulose Part1: Introduction of amino groups on C and N atoms

Jianwei Zhang[a,b], Chengming Bian[c], Ling Chen [a,b], Weidong He[a,b*]

[a] School of Chemistry and Chemical Engineering, Nanjing University of Science and Technology, Nanjing, Jiangsu, 210094, China;

[b] Key Laboratory of Special Energy Materials, Ministry of Education, Nanjing, Jiangsu, 210094, China;

[c] School of Chemistry and Chemical Engineering, North University of China, Taiyuan, Shanxi, 030051, China;

Corresponding Email: hewedong@njust.edu.cn

S1. Materials

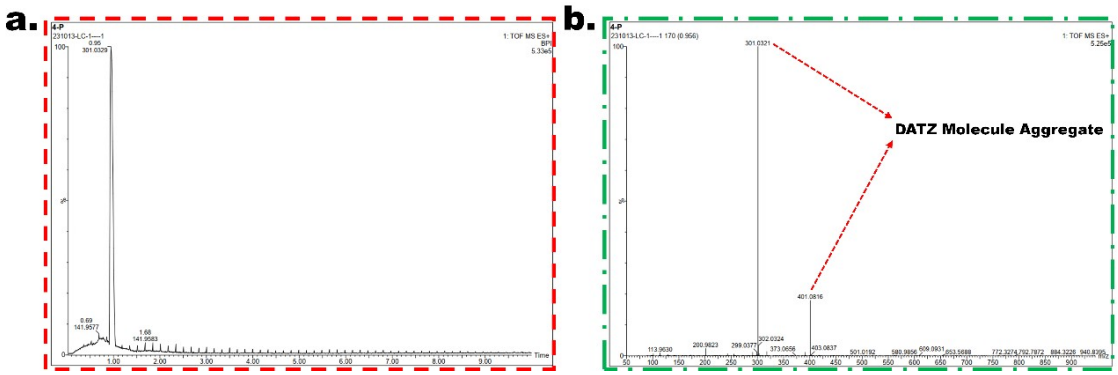

Fig.S1 The HPLC-MS analysis results of DATZ.

S2. The gas products analysis of 5-ATZ and DATZ

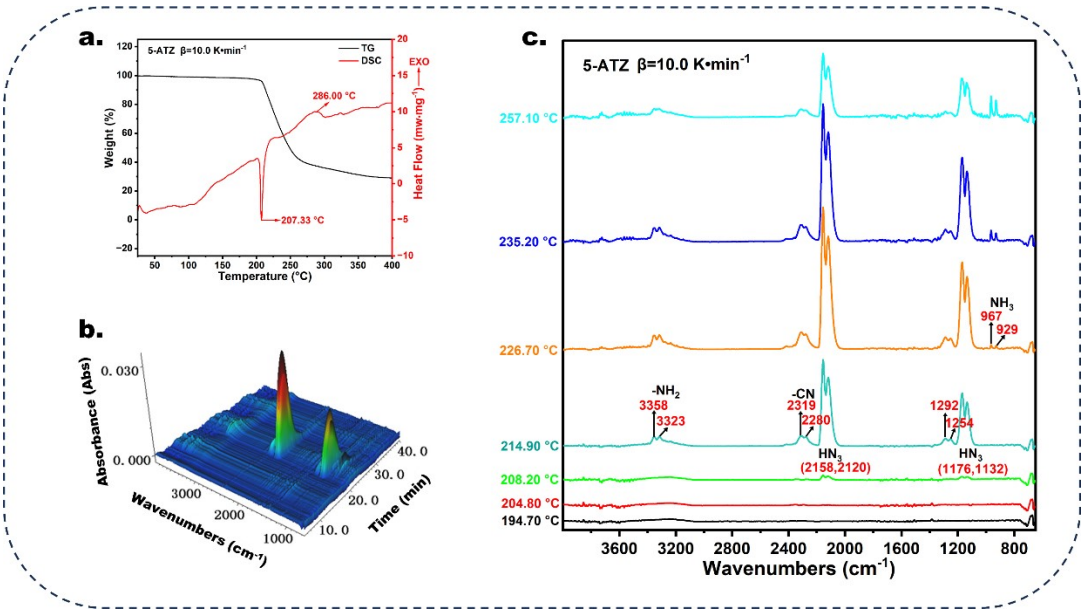

Fig.S2 The pyrolysis process of 5-ATZ： TG-DSC curves at the heating rate of 10.0 K•min^{-1} (a.), 3D images (b.) and the characteristic absorption of pyrolysis gas (c.)

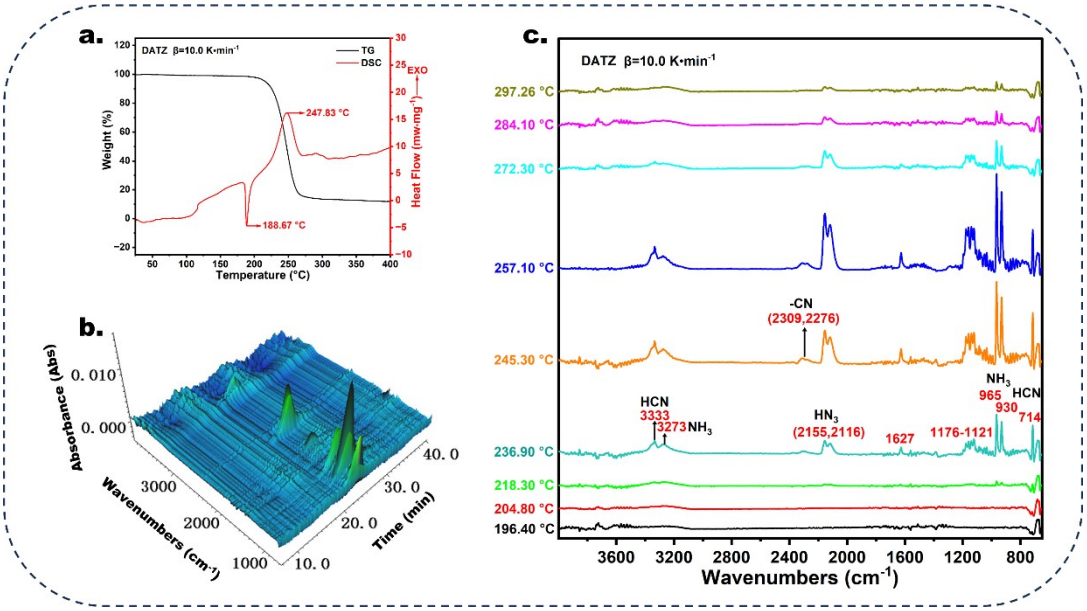

Fig.S3 The pyrolysis process of DATZ： TG-DSC curves at the heating rate of 10.0 K•min^{-1} (a.), 3D images (b.) and the characteristic absorption of pyrolysis gas (c.)

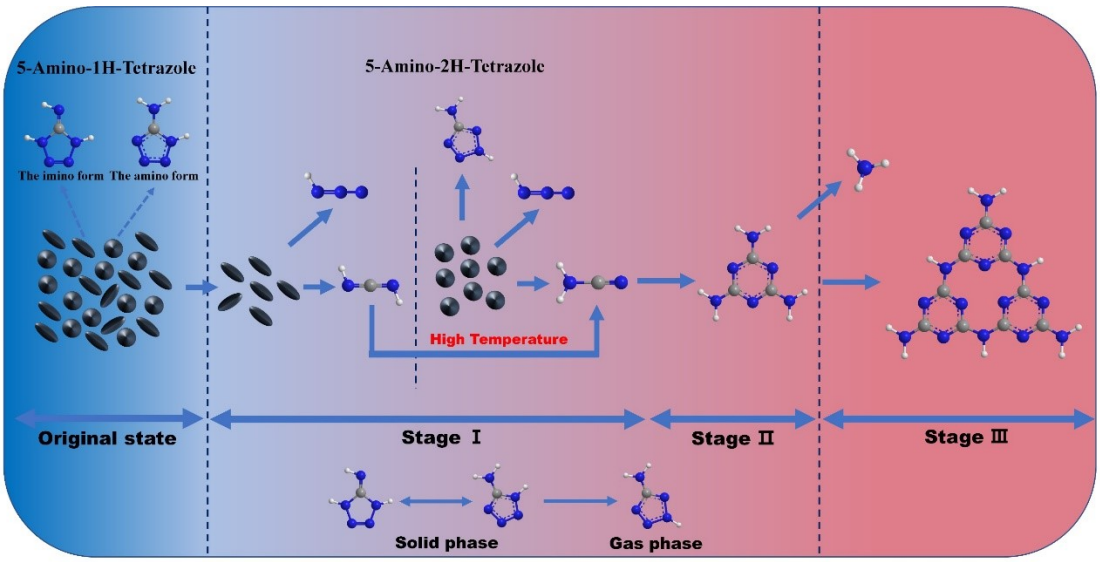

Fig.S4 The pyrolysis mechanism of 5-ATZ.

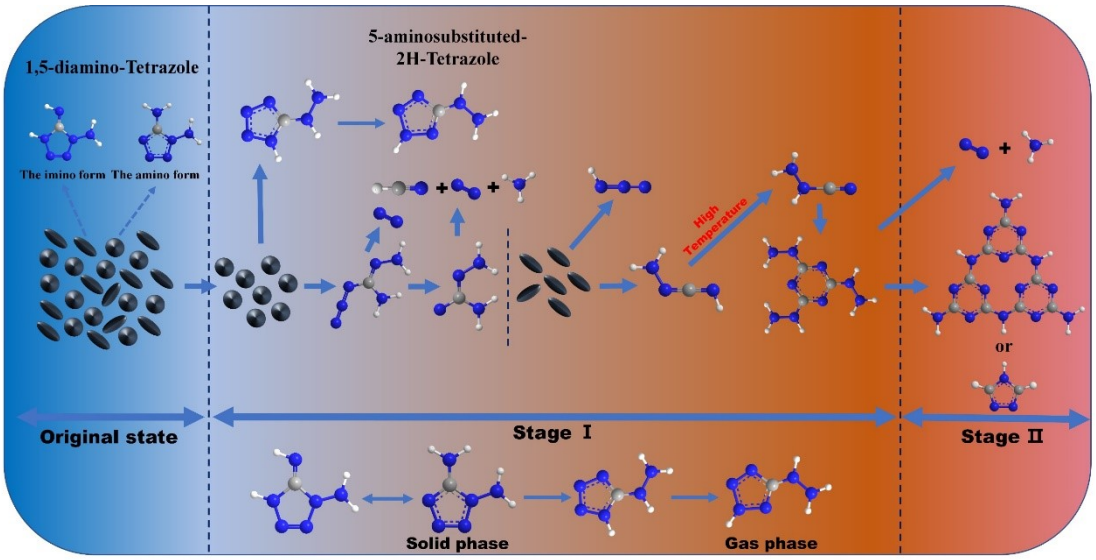

Fig.S5 The pyrolysis mechanism of DATZ.

S3. The variation of the E_a analysis

TableS1 During the thermal decomposition process of 5-ATZ+NC, the variation of the E_a with conversion α within open environment and the correlation coefficient R^2 at different conversion α.

Conversion	The E_a was calculated by Friedman method				The E_a was calculated by KAS method			
α	region①	R^2	Region②	R^2	Region①	R^2	Region②	R^2
0.10	166.91	0.9983	180.08	0.9970	192.68	0.9993	162.90	0.9997
0.15	166.48	0.9980	181.37	0.9978	187.28	0.9999	164.31	0.9993
0.20	160.70	0.9971	186.31	0.9980	182.22	0.9999	166.42	0.9995
0.25	157.14	0.9966	188.34	0.9974	178.50	0.9998	167.37	0.9991
0.30	155.24	0.9969	190.64	0.9967	176.12	0.9997	168.04	0.9996
0.35	154.51	0.9970	188.48	0.9923	174.33	0.9995	167.95	0.9991
0.40	154.94	0.9979	187.97	0.9847	172.61	0.9998	169.48	0.9985
0.45	157.04	0.9971	184.96	0.9771	171.97	0.9995	171.19	0.9988
0.50	157.86	0.9981	178.65	0.9589	170.40	0.9997	171.05	0.9978
0.55	159.09	0.9971	170.39	0.9459	169.72	0.9993	171.24	0.9957
0.60	161.57	0.9974	166.30	0.9553	169.70	0.9993	173.04	0.9935
0.65	162.66	0.9971	162.36	0.9770	168.05	0.9991	169.04	0.9925
0.70	165.95	0.9977	166.57	0.9868	168.62	0.9995	168.53	0.9899
0.75	168.46	0.9964	169.84	0.9930	167.95	0.9991	170.33	0.9911
0.80	173.18	0.9970	166.50	0.9931	168.65	0.9995	168.91	0.9925
0.85	176.68	0.9951	163.69	0.9873	168.05	0.9991	169.20	0.9913
0.90	170.80	0.9994	163.48	0.9776	168.05	0.9991	167.32	0.9900

TableS2 During the thermal decomposition process of 5-ATZ+NC, the variation of the E_a with conversion α within closed environment and the correlation coefficient R^2 at different conversion α.

Conversion	The E_a was calculated by Friedman method				The E_a was calculated by KAS method			
α	region①	R^2		region①	R^2		region①	R^2
0.10	132.02	0.9991	129.00	0.9987	158.61	0.9867	136.01	0.9990
0.15	128.32	0.9993	128.92	0.9980	151.86	0.9939	136.25	0.9987
0.20	121.90	0.9999	128.38	0.9980	146.48	0.9952	136.01	0.9990
0.25	120.62	0.9997	127.74	0.9976	144.58	0.9970	135.95	0.999
0.30	124.67	0.9996	126.06	0.9965	141.17	0.9981	134.88	0.9987
0.35	133.81	0.9978	124.33	0.9966	139.63	0.9979	133.90	0.9991
0.40	138.63	0.9976	123.32	0.9944	140.03	0.9987	133.73	0.9983
0.45	138.92	0.9971	120.93	0.9943	139.40	0.9992	132.85	0.9988
0.50	138.66	0.9974	119.01	0.9926	139.40	0.9992	132.41	0.9983
0.55	138.06	0.9970	116.77	0.9924	139.75	0.9996	132.35	0.9983
0.60	135.70	0.9972	113.62	0.9907	139.75	0.9996	131.28	0.9979
0.65	132.19	0.9969	110.06	0.9890	138.62	0.9994	130.19	0.9973
0.70	130.32	0.9981	104.78	0.9903	139.33	0.9991	129.21	0.9979
0.75	127.58	0.9981	96.69	0.9930	138.62	0.9994	126.14	0.9980
0.80	125.49	0.9985	88.28	0.9955	137.21	0.9993	123.82	0.9975
0.85	124.31	0.9982	77.25	0.9983	136.48	0.9994	120.01	0.9971
0.90	124.91	0.9978	64.63	0.9813	137.47	0.9991	113.17	0.9968

TableS3 During the thermal decomposition process of DATZ+NC, the variation of the E_a with conversion α within open environment and the correlation coefficient R^2 at different conversion α.

Conversion	The E_a was calculated by Friedman method				The E_a was calculated by KAS method			
α	region①	R^2	Region②	R^2	Region①	R^2	Region②	R^2
0.10	156.46	0.9801	137.22	0.9866	117.66	0.9776	146.50	0.9970
0.15	167.00	0.9491	133.45	0.9840	123.66	0.9904	146.31	0.9958
0.20	172.50	0.9646	129.36	0.9811	127.69	0.9960	145.44	0.9950
0.25	176.06	0.9878	125.43	0.9801	131.22	0.9982	143.91	0.9955
0.30	178.01	0.9921	122.99	0.9772	135.03	0.9988	143.82	0.9955
0.35	175.76	0.9905	118.26	0.9687	136.55	0.9994	141.28	0.9938
0.40	174.89	0.9906	115.22	0.9623	139.18	0.9996	141.23	0.9937
0.45	172.74	0.9894	109.79	0.9525	140.96	0.9992	138.88	0.9934
0.50	170.35	0.9894	103.67	0.9292	142.43	0.9989	137.40	0.9907
0.55	168.80	0.9898	94.68	0.8956	144.80	0.9991	134.03	0.9893
0.60	164.29	0.9867	84.85	0.8426	144.76	0.9983	131.49	0.9887
0.65	160.57	0.9862	73.39	0.7520	145.15	0.9984	127.74	0.9827
0.70	157.65	0.9841	63.38	0.6815	146.27	0.9981	121.52	0.9769
0.75	154.62	0.9821	57.54	0.6617	147.48	0.9976	115.36	0.9705
0.80	149.16	0.9814	54.11	0.6969	146.20	0.9969	109.37	0.9630
0.85	145.12	0.9826	53.89	0.8450	146.20	0.9969	102.64	0.9561
0.90	141.39	0.9840	57.86	0.9977	146.20	0.9969	95.87	0.9583

TableS4 During the thermal decomposition process of DATZ+NC, the variation of the E_a with conversion α within closed environment and the correlation coefficient R^2 at different conversion α.

Conversion	The E_a was calculated by Friedman method				The E_a was calculated by KAS method			
α	region①	R^2		region①	R^2		region①	R^2
0.10	101.67	0.9854	126.36	0.9949	139.45	0.9836	134.33	0.9970
0.15	97.18	0.9895	124.14	0.9946	126.13	0.9826	133.24	0.9965
0.20	136.49	0.9746	122.65	0.9950	126.16	0.9884	132.28	0.9972
0.25	146.21	0.9923	122.20	0.9938	127.40	0.9909	132.48	0.9967
0.30	151.17	0.9995	120.70	0.9939	129.10	0.9943	131.64	0.9973
0.35	152.95	0.9975	120.46	0.9941	131.78	0.9950	131.60	0.9973
0.40	151.49	0.9966	119.14	0.9927	133.30	0.9965	130.87	0.9972
0.45	147.76	0.9946	117.98	0.9935	133.67	0.9964	130.46	0.9967
0.50	145.07	0.9941	116.54	0.9930	135.05	0.9966	129.96	0.9976
0.55	141.31	0.9939	114.31	0.9919	135.04	0.9966	128.90	0.9971
0.60	136.51	0.9947	111.70	0.9910	135.05	0.9966	127.85	0.9965
0.65	132.95	0.9948	108.44	0.9907	135.46	0.9975	126.90	0.9970
0.70	129.74	0.9956	103.61	0.9889	135.01	0.9967	125.07	0.9968
0.75	127.09	0.9948	98.79	0.9880	134.40	0.9971	123.84	0.9970
0.80	126.35	0.9952	92.83	0.9820	134.33	0.9970	121.42	0.9963
0.85	126.60	0.9951	85.68	0.9651	134.78	0.9977	118.63	0.9954
0.90	125.48	0.9945	78.71	0.8899	133.71	0.9972	113.68	0.9970

S4. The variation of the E_a of NC

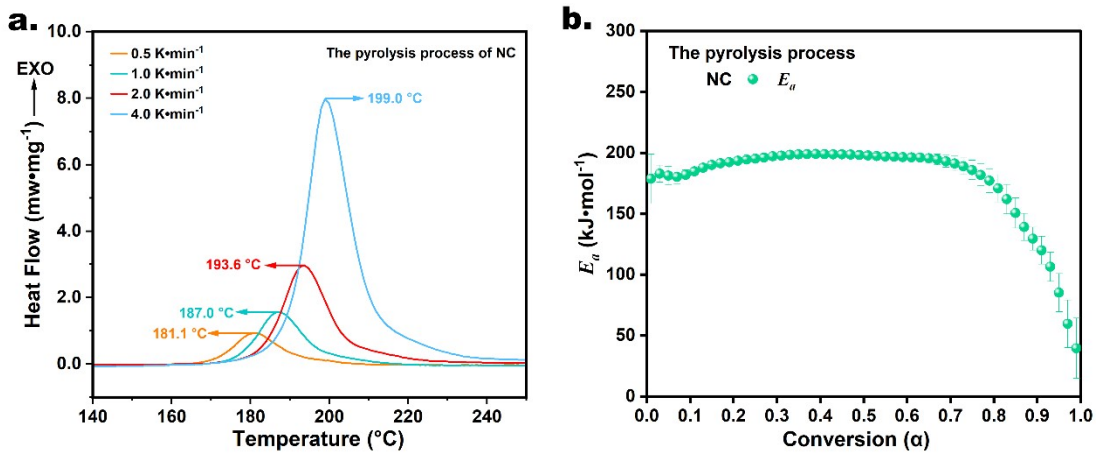

Fig.S6 NC thermal decomposition process: a. DSC curves at different heating rates and b. The E_a changed with conversion α.

DSC tests of NC were performed using aluminum crucible with a pinhole. DSC curves of NC at the heating rate of 0.5, 1.0, 2.0, 4.0 K•min^{-1} were shown in **Fig.S6a**. The E_a at different conversion α was shown in **Fig.S6b**. During the thermal decomposition process of NC, the E_a increased slowly from 178.66 kJ•mol^{-1} to 199.06 kJ•mol^{-1} when the conversion α was less than 0.4. When the conversion α was greater than 0.4 but less than 0.7, the E_a slowly decreased from 199.06 kJ•mol^{-1} to 192.27 kJ•mol^{-1}. When the conversion α was greater than 0.7, the E_a gradually decreased from 192.27 kJ•mol^{-1} to 39.51 kJ•mol^{-1}.

S5. Kinetics model analysis

TableS5 The characteristic parameters of Peak1 and Peak2 in the thermal decomposition process of 5-ATZ and NC mixture in a closed environment by Fityk software using the Fraser-Suzuki function.

β (K•min^{-1})	Peak Index	H_p	T_p	W_{hf}	A_s	Area（%）	R^2
0.5	1	0.29	165.39	31.37	0.04	44.33	0.9978
	2	0.97	171.12	11.83	-0.04	55.67	
1.0	1	0.73	173.28	32.19	0.04	44.00	0.9990
	2	2.54	178.49	11.79	-0.04	56.00	
2.0	1	1.20	182.10	34.47	0.04	42.84	0.9989
	2	4.40	186.45	12.56	-0.04	57.16	
4.0	1	1.94	193.63	40.51	0.04	48.65	0.9992
	2	5.91	195.08	13.97	-0.04	51.35	

TableS6 The characteristic parameters of Peak0, Peak1 and Peak2 in the thermal decomposition process of DATZ and NC mixture in a closed environment by Fityk software using the Fraser-Suzuki function.

β (K•min^{-1})	Peak Index	H_p	T_p	W_{hf}	A_s	Area（%）	R^2
0.5	0	-0.16	163.25	4.76	-0.04	-	0.9990
	1	0.22	168.32	27.14	-0.07	30.09	
	2	1.12	169.60	12.55	-0.02	69.91	
1.0	0	-0.17	168.33	5.29	-0.04	-	0.9992
	1	0.31	182.52	45.37	-0.07	33.60	
	2	1.89	176.52	14.66	-0.02	66.40	
2.0	0	-0.78	174.99	5.57	-0.04	-	0.9998
	1	0.59	191.42	50.75	-0.07	27.20	
	2	5.24	184.62	14.97	-0.02	72.80	
4.0	0	-0.91	180.36	5.85	-0.04	-	0.9998
	1	1.02	200.24	42.51	-0.07	31.16	
	2	5.69	194.02	16.79	-0.02	68.84	

TableS7 During thermal decomposition process of NC，the optimize parameters of kinetic model.

Kinetic model \ Optimize parameters			R^2	S^2	MR	F-Test
Friedman method			0.99760	3.442	0.030	5.702
Kinetic model	A→B	B→C				
A→B→C	C_n	F_n	0.99938	0.891	0.020	1.188
	$C_{n,m}$	F_n	0.99948	0.749	0.018	1.000

TableS8 During thermal decomposition process of the mixture of 5-ATZ and NC，the optimize parameters of kinetic model of Peak2.

Kinetic model \ Optimize parameters			R^2	S^2	MR	F-Test
Friedman method			0.98599	58.035	0.095	16.522
Kinetic model	A→B	B→C				
A→B→C	C_n	F_n	0.99727	11.384	0.052	2.843
	$C_{n,m}$	F_n	0.99904	4.002	0.032	1.000

TableS9 During thermal decomposition process of the mixture of DATZ and NC，the optimize parameters of kinetic model of Peak2.

Kinetic model \ Optimize parameters			R^2	S^2	MR	F-Test
Friedman method			0.99689	15.763	0.053	2.175
Kinetic model	A→B	B→C				
A→B→C	C_n	F_n	0.99678	16.301	0.067	1.976
	$C_{n,m}$	F_n	0.99837	8.245	0.042	1.000

S6. The thermal decomposition process of NC

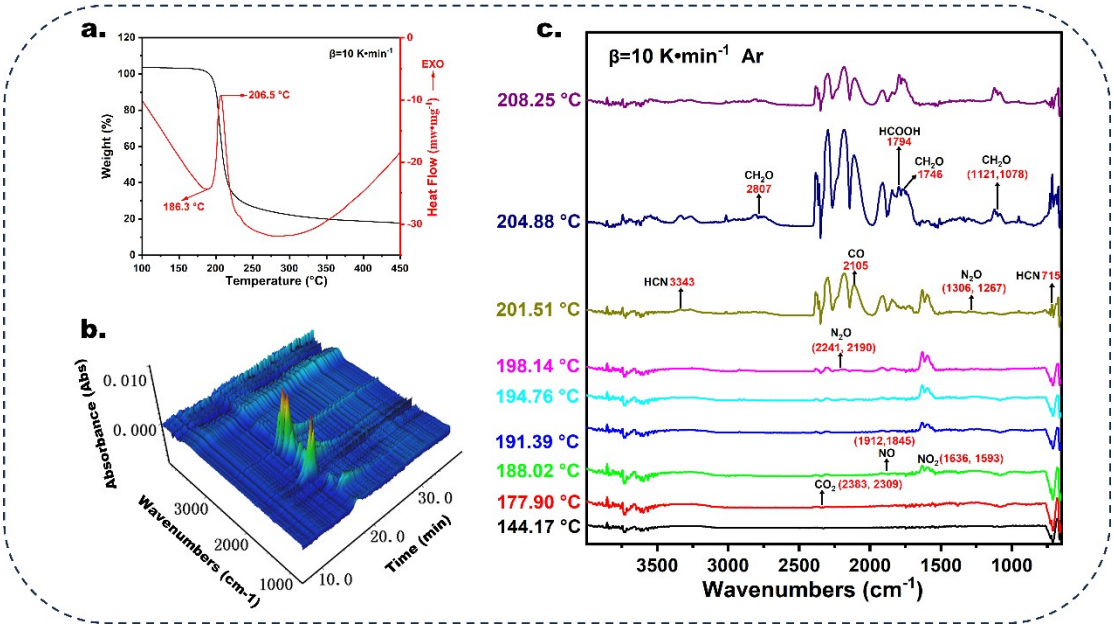

Fig.S7 The thermal decomposition process of NC at the heating rate of 10.0 K•min^{-1}: (a.) TG-DSC curves, (b.) 3D images and (c.) the characteristic absorption of pyrolysis gas.

Form the DTG curve in **Fig.S7a**, it can be observed that the NC became decompose at 186.3 °C and its corresponding peak temperature was 206.5 °C. Based on the decomposition parameters of NC, the decomposition gaseous products were collected and detected by IR and the 3D images as well as its corresponding absorption peaks were obtained, as shown in **Fig.S7b** and **Fig.S7c**. As displayed, the infrared absorption peak of CO_2 (2383 cm^{-1}, 2309 cm^{-1}) can be observed at 177.90 °C. Subsequently, the infrared absorption peaks of NO (1912 cm^{-1}, 1845 cm^{-1}) and NO_2 (1636 cm^{-1}, 1593 cm^{-1}) can be observed at 188.02 °C. The above phenomenon showed that -O-NO_2 bond of NC was broken firstly, forming -HC=O group and NO_2. Meanwhile, NO_2 was retained in the fiber skeleton to further oxidize the residue and accelerate the breakage of the remaining -O-NO_2 bond, inter-ring C-O-C bond and intra-ring oxygen bridges. After then, the products of NO_2, NO, N_2O (2241 cm^{-1}, 2190 cm^{-1}, 1306 cm^{-1}, 1267 cm^{-1}), CO (2105 cm^{-1}), CO_2, CH_2O (2807 cm^{-1}, 1746 cm^{-1}, 1123 cm^{-1}, 1073 cm^{-1}) and other gases were released further. After the breakage of most of -O-NO_2, the residue further was decomposed, releasing HCOOH (1794 cm^{-1}) and HCN (715 cm^{-1}, 3343 cm^{-1})[1]. Based on above TG-DSC-FTIR results, the thermal decomposition mechanism of the NC was inferred to be a three-step process, as shown in **Fig.S8**.

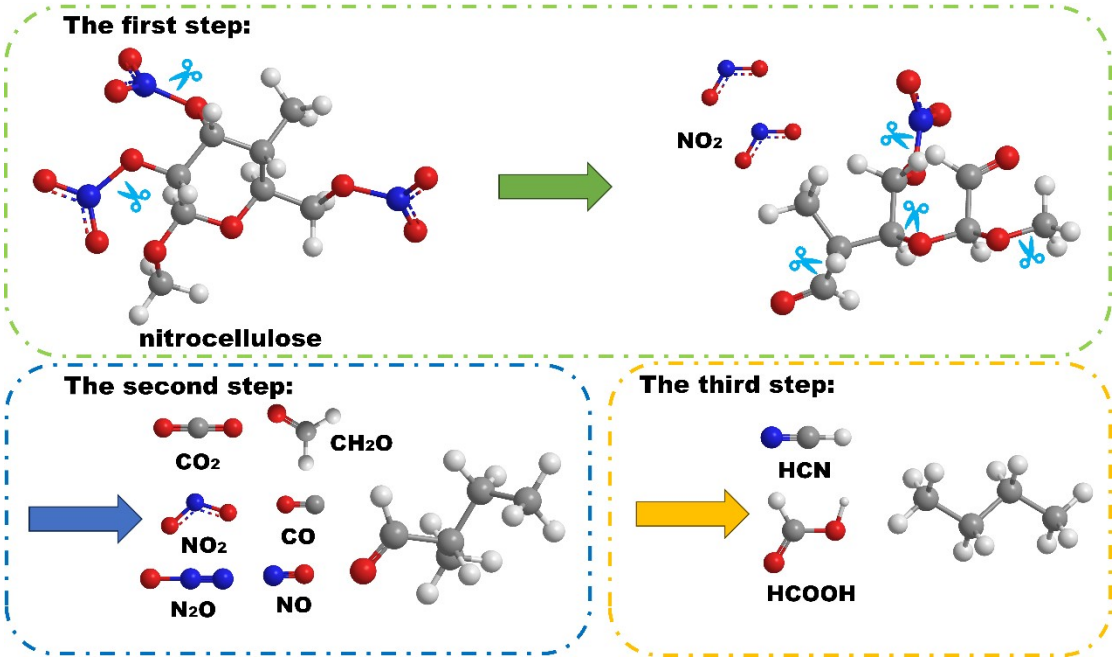

Fig.S8 Thermal decomposition mechanism of NC.